



HAL
open science

From single III-nitride nanowires to piezoelectric generators: New route for powering nomad electronics

Noëlle Gogneau, Nicolas Jamond, Pascal Chrétien, Frédéric Houzé, Elie Lefeuvre, M Tchernycheva

► To cite this version:

Noëlle Gogneau, Nicolas Jamond, Pascal Chrétien, Frédéric Houzé, Elie Lefeuvre, et al.. From single III-nitride nanowires to piezoelectric generators: New route for powering nomad electronics. Semiconductor Science and Technology, 2016, 31, pp.103002. 10.1088/0268-1242/31/10/103002 . hal-01390955

HAL Id: hal-01390955

<https://hal.science/hal-01390955v1>

Submitted on 2 Nov 2016

HAL is a multi-disciplinary open access archive for the deposit and dissemination of scientific research documents, whether they are published or not. The documents may come from teaching and research institutions in France or abroad, or from public or private research centers.

L'archive ouverte pluridisciplinaire **HAL**, est destinée au dépôt et à la diffusion de documents scientifiques de niveau recherche, publiés ou non, émanant des établissements d'enseignement et de recherche français ou étrangers, des laboratoires publics ou privés.

From Single III-Nitride Nanowires to Piezoelectric Generators: New Route for Powering Nomad Electronics

N. Gogneau^{1*}, N. Jamond¹, P. Chrétien², F. Houzé², E. Lefeuvre³, M. Tchernycheva^{3*}

¹ Laboratoire de Photonique et de Nanostructures, CNRS, Université Paris-Saclay, Route de Nozay, F-91460 Marcoussis, France

² Laboratoire de Génie Électrique et Électronique de Paris (GeePs), UMR 8507 CNRS-Centrale Supélec, Paris-Sud et UPMC Université, 11 rue Joliot-Curie, Plateau de Moulon, 91192 Gif-sur-Yvette, France

³ Institut d'Electronique Fondamentale, CNRS UMR 8622, Université Paris-Saclay, 91405 Orsay, France

Corresponding authors' emails : noelle.gogneau@lpn.cnrs.fr ; maria.tchernycheva@u-psud.fr

Keywords : GaN nanowires, Piezoelectric properties, Energy harvesting, Nanogenerators, Piezogenerators

Abstract

Ambient energy harvesting using piezoelectric nanomaterials is today considered as a promising way to supply microelectronic devices. Since the first demonstration of electrical energy generation from piezoelectric semiconductor nanowires in 2006, the piezoelectric response of 1D-nanostructures and the development of nanowire-based piezogenerators have become a hot topic in nanoscience. After several years of intense research on ZnO nanowires, III-nitride nanomaterials have started to be explored thanks to their high piezoelectric coefficients and their strong piezo-generation response. This review describes the present status of the field of piezoelectric energy generation with nitride nanowires. After presenting the main motivations and a general overview of the domain, a short description of the main properties of III-nitride nanomaterials is given. Then we review the piezoelectric responses of III-N nanowires and the specificities of the piezo-generation mechanism in these nanostructures. Finally, the design and performance of the macroscopic piezogenerators based on nitride nanowire arrays are described, showing the promise of III-nitride nanowires for ultra-compact and efficient piezoelectric generators.

Introduction

Portable electronic equipment such as biomedical devices, portable multimedia, distributed sensor networks or mobile communication are omnipresent in our daily life and the question concerning their autonomy is a key societal challenge. Electronic devices have known a tremendous progress in the past decades with the development of systems at micrometer and even nanometer scale. The device miniaturization in particular results in the reduction of their energy consumption going down to milliWatt and even microWatt. Despite the recent progress in the development of batteries with high energy density [Arma2009; Mill2008] as well as of nanobatteries, these sources are not ideally suited to supply electronic microdevices since they present limitations such as complex integration, limited capacity and considerable cost. In this context, new competitive ultra-compact and integrable electrical sources should be developed generating sufficient power to supply the microdevices without increasing microsystem size and adding weight.

Energy harvesting, i.e. conversion of the ambient energy found in the vicinity of the device into usable electrical energy, appears as the most promising way for powering wireless microdevices. Among the alternative sustainable energy resources, the mechanical deformations and vibrations present the advantages to be ubiquitously available at all time and more accessible than solar and thermal energy. The vibration energy may have various origins such as body movements, sound vibrations, hydraulic movements, wind, friction.... Harvesting of this energy through the use of piezoelectric materials has received these last years a great attention due to the abilities of these materials to convert mechanical deformation directly into electrical energy.

Piezoelectric energy harvesting is not a new concept. It has been practiced for decades at the macroscopic scale and commercialized. The most common application of piezoelectric materials is the fabrication of sensors and actuators, however their use as electrical generators remains until now rather limited (the best-known applications are the quartz used in watches or the electric cigarette lighter). Indeed, the power output from conventional bulk piezoelectric ceramics is low. In addition, bulk materials are not well suited for energy harvesting applications since they are massive, not easily integrable and their sensitivity to ambient mechanical vibrations is very weak. To increase the sensitivity to the applied force and thus the conversion efficiency, micro-structured piezo-composite materials such as for example 1-3 connected ceramic-polymer composites have been developed [Chan2005]. However, the fiber diameter in these materials (tens to hundreds microns) remained rather big. With the development of nanotechnologies, it has been shown that further downscaling of the fiber dimensions, i.e. their replacement by nanowires (NWs), can significantly enhance the conversion efficiency.

Semiconductor nanowires presenting piezoelectric properties have recently emerged as excellent candidates to fabricate novel ultra-compact and efficient piezoelectric generators. Due to their specific structural properties, these 1D-nanostructures can enhance the piezoelectric properties of the material compared to its bulk or 2D form. In particular, the NWs present superior mechanical properties. Due to the structural perfection of NWs, resulting in absence of defects, such as dislocations, they can be subject to large elastic deformation without plastic deformation or fracture [Yang2010]. They are also characterized by higher flexibility, higher robustness and higher resistance to fatigue, which extend the operational lifetime of the piezogenerator. The NWs can be bended under an extremely small applied force due to the small diameter and the large aspect ratio characterizing these 1D-nanostructures. Hence, it is possible to generate a

significant strain in the NWs under pico/nano-Newton applied forces [Zhou2012]. Finally, as illustrated in Table 1, quasi-1D geometry results in an enhancement of the piezoelectric coefficients in comparison with their bulk counterparts, due to surface effects [Zhao2004; Agra2011; Mina2012].

Table 1. Piezo coefficient d_{33} (pm/V) for low-dimensional and bulk GaN and ZnO.

Material	Low-dimensional	Bulk
ZnO	14.3-26.7 [Zhao2004]	9.93 [Zhao2004]
GaN	12.4 [Mina2012]	2.8-3.7 [Guy1999]

The first electricity generation from the mechanical deformation of ZnO NWs has been demonstrated by the group of Prof. Wang from the Georgia Institute of Technology in USA [Wang2006]. Since this first demonstration, several 1D-nanostructures including nanostructured conventional piezoceramics have been studied, such as CdS [Lin2008], CdSe [Zhou2012b], PZT [Chen12], BaTiO₃ [Wang2010], etc. Despite their strong piezoelectric response [Bern1997], III-nitride nanostructures have been much less studied compared to ZnO. These materials, crystallizing in wurtzite phase with hexagonal structure, are characterized by a strong internal electric field, which results from the combination of the spontaneous and piezoelectric polarizations. The first electric generation resulting from the deformation of a GaN nanorod has been evidenced in 2007 by Su et al. [Su2007]. The investigation of piezoelectric properties of GaN nanowires was then continued by different groups [Xu2010; Huan2010b; Xu2011; Gogn2014]. Other nitride NW materials than GaN were investigated, namely AlN, AlGaIn [Wang2010b] and InN [Ku2012; Huan2010]. Up to now, the best mechanical-electrical conversion from NWs in terms of the output voltage has been obtained with GaN and InN NWs, with a maximum generated voltage per nanowire of about 440 mV [Gogn2014] and 1 V [Huan2010], respectively. These output voltages measured from single piezoelectric III-N NWs are larger than those for other piezoelectric semiconductors, and in particular ZnO NWs, which is today the most widely used material in nanostructure-based piezo-generation and whose output voltages do not exceed 45 mV [Gao2007] and 80 mV [Lu2009] for respectively n-doped and p-doped materials.

It should be noted that semiconductor NWs such as ZnO or nitrides differ from conventional piezoceramics by the presence of free charges (controlled by doping), which impact the piezoconversion. From the theoretical viewpoint, Finite Element Method is usually used to analyze piezoconversion with semiconductor NWs and in particular to predict the electric potential resulting from their deformation (see for example [Hinc2014]).

The studies of piezoelectric properties of individual semiconductor NWs have naturally lead to the development of macroscopic NW-based piezo-generators. To avoid confusion existing in the literature, in this review we define a “nanogenerator” as a single nanowire producing electricity via piezo effect, while we call “nanowire-based piezogenerator” a macroscopic device based on a nanowire array. The first prototype of an integrated piezogenerator realized by Prof. Wang’s group was based on a single layer of ZnO NWs and exhibited an operational power output of approximately 2.5 nW/cm² [Wang2007]. Subsequent realizations have significantly improved the performance of the ZnO-based piezo-generators. Three different configurations have been introduced: the Lateral nanowire Integrated Nanogenerator (LING) [Xu2010], the Nanocomposite Electrical Generators (NEG) [Mome2010] and the Vertical nanowire Integrated Nanogenerator (VING) [Xu2008]. The interest of the use of flexible substrates to fabricate nanogenerators has been first evidenced by a new prototype based on cyclic stretching/releasing

of a single piezoelectric wire packaged on a flexible substrate. Such nanogenerator configuration producing an AC output voltage of around 50 mV has been reported as very attractive for harvesting biomechanical energy [Yang2009]. The advantage of this flexible support has been combined to the VING configuration in order to increase the generator performance. An output power density of the order of several hundred of mW/cm^3 was reported [Zhu2012].

A fundamental difference should be noted between NW piezo-generators and piezoelectric Micro Electro Mechanical Systems (MEMS). MEMS operate in a resonant mode (with a typical resonance frequency in the MHz range), which is not efficient for energy harvesting from ambient vibration sources, which are either non periodic or have a low frequency (typically below 200 Hz). On the contrary, the enhanced flexibility of NWs enables the operation of NW generators in a quasi-static regime, so that the amount of converted energy is determined not by the operating frequency but by the number of active NWs [Ardi2012].

From ZnO NWs based piezo-generator prototypes, self-powered nano-systems without external battery have been demonstrated including pH, UV [Xu2010], chemical [Li2010] and biological sensors [Lee2011], commercial or nanostructured light-emitting diodes (LED) [Zhu2010, Chen2012b], liquid-crystal-display (LCD) screen [Hu2011] or wireless radio frequency data transmitter [Hu2011b]. Finally, piezo-generators based on ZnO NWs have been applied to self-powered nanodevices for in vivo biomedical applications by harvesting biochemical energy [Pan2010] or a combination of biomechanical and biochemical energy [Pan2011; Hans2010; Lee2014].

Although ZnO NWs remain today the dominant material investigated for the development of NW piezogenerators, the field has been extended to other materials such as PVDF [Chan2010] or PZT nanofibers [Chen2010]. Concerning III-nitride nanostructures, to the best of our knowledge, only few macroscopic piezo-generators based on nitride NWs have been reported in the literature. The first prototype consists of multiple layers of dispersed NWs embedded in polymethyl methacrylate (PMMA) [Lin2011], while the second one is based on vertical aligned InN NWs [Liu2016], both generators exhibiting respectively an output power density of $\sim 0.3 \text{ mW}/\text{cm}^3$ and $\sim 0.15 \text{ mW}/\text{cm}^3$ (calculated from the published data). Finally, the third piezogenerator integrating a vertical array of GaN NWs was reported to generate a power density of the order of $12.7 \text{ mW}/\text{cm}^3$, which approaches the best values reported for ZnO NW based piezogenerators [Zhu2012]. Piezoelectric properties of nitride NWs have also been used for other applications than energy harvesting. For example, high sensitivity pressure sensors based on GaN NWs have been reported [Zhou2013; Salo14]. In general, the interplay between the semiconducting and piezoelectric properties in nanostructures receives today an increasing attention since it offers new interesting functionalities [Wen2015].

It should be noted that there is no consensus in the literature on how to evaluate the generated power of a NW-based generator in a normative way. The electrical performance is either given in absolute values or is normalized with respect to the generator volume or surface area. Different electrical load circuits are used, so that comparison between different reports is not straightforward. In this review, when the generated power is not given, we try to estimate it from the parameters provided in the publications where it is possible.

Numerous realizations show the capability of NW piezogenerators to produce electrical power in $\mu\text{W} - \text{mW}$ range. Their use for energy harvesting thus appears as a very promising concept for realizing self-powered microelectronics. However, the optimization of the mechanical-electrical

conversion of individual nanowires and of the macroscopic generator architecture are crucial issues for the development of efficient devices. In this review, we address the status of these two technological challenges restricting ourselves to the specific case of III-nitride nanowires. After a short description of the main properties of III-nitride nanomaterials for the piezo-generation in section 1, the piezoelectric responses of III-N NWs and the analyses of the piezo-generation mechanism are presented in section 2. Section 3 is dedicated to the overview of the existing piezo-generators based on nitride NW arrays.

1- III-Nitride NWs.

III-nitride nanowires have been intensively studied from the early years 2000. The strong interest to these nanomaterials has been mainly stimulated by their numerous optoelectronic applications, in particular for light emission. Nitride nanowires can be elaborated by different growth techniques, the most widespread ones are Chemical Vapor Deposition (CVD), Molecular Beam Epitaxy (MBE) and Metal Organic Vapor Phase Epitaxy (MOVPE). III-N nanowires grown by MBE are particularly interesting for piezogeneration since this technique allows for an ultimate control over the nanowire properties such as their size, aspect ratio, doping level, etc. In addition, NWs with diameters as small as 20 nm can be achieved as illustrated in Fig 1.

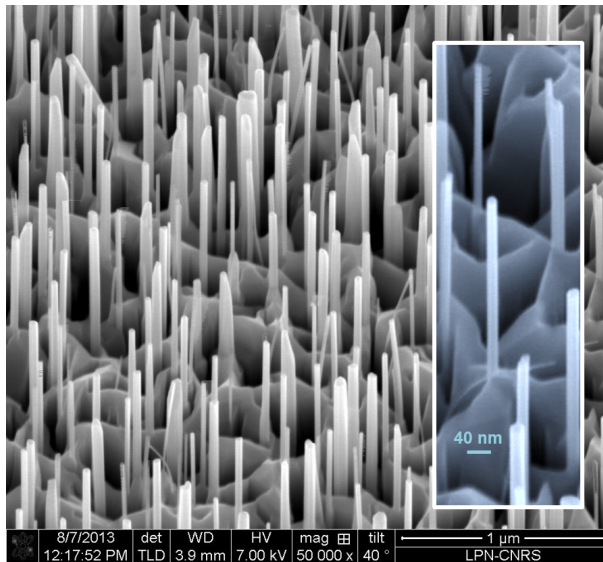


Fig. 1: SEM image of GaN NWs grown by MBE. Inset displays a high magnification image showing NWs with a diameter as low as 20 nm.

III-nitride nanowires crystallize in wurtzite structure, where the cations and anions form a tetrahedral coordination. The III-N materials are characterized by the absence of inversion symmetry, which confers them two important characteristics. The first one is the presence of polar surfaces with the metal-terminated (0001) and the N-terminated (000-1) orientation (Fig. 2). These two faces are not equivalent and present different properties, such as different surface morphologies, optical and kinetic properties [Feen2002, Huan2002, Jang2002]. The second characteristic is the existence of an internal polarization along the z-axis. This one consists of the sum of the spontaneous polarization (P_{SP}) and of the piezoelectric polarization (P_{PZ}). When the hexagonal structure is at equilibrium, *i.e.* not subjected to an external deformation, the centroids

of positive and negative charges do not coincide. This results in the formation of a set of dipoles oriented along the same direction, leading to the appearance of a macroscopic polarization in the material, so-called spontaneous polarization. P_{SP} is aligned with the z axis and oriented from N to Ga atoms. Thus P_{SP} is parallel to the (000-1) growth direction and anti-parallel to the (0001) growth direction as illustrated on figure 2. The piezoelectric polarization results from the relative displacement of the Ga cations with respect to the N anions along the deformation direction when a stress is applied to the material. Its orientation along the z axis is driven both by the P_{PS} orientation and by the strain created inside the materials. Hence, under axial compression, P_{PZ} is oriented anti-parallel to the P_{PS} , while it is parallel to the P_{PS} , under axial stretching.

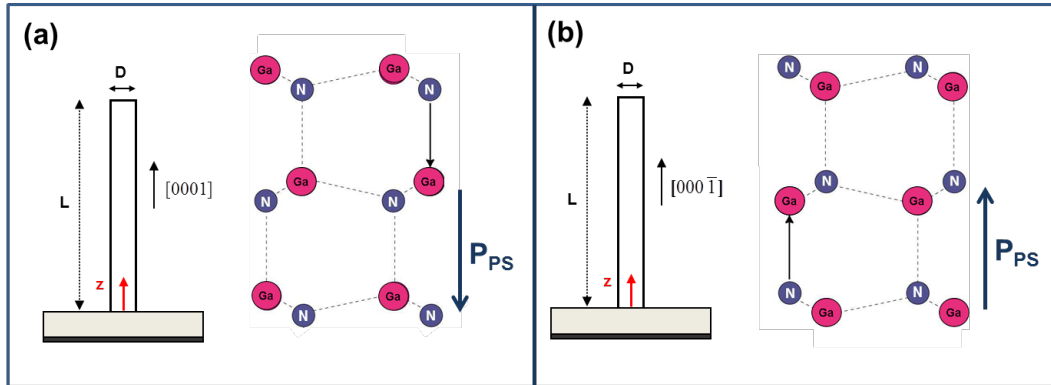


Fig. 2: Representation of the GaN structure for Ga-face (a) and N-face (b). The orientation of the spontaneous polarization is given as a function of the structure polarity.

2- Piezoelectric properties of III-N NWs.

The performance of a piezoelectric energy harvesting system primarily depends on the piezoelectric properties of the material used to fabricate the generators. For this reason, it is of great importance to quantify the mechanical-electrical conversion efficiency and the achievable output power of NWs as a function of their structural and electric characteristics.

One of the most common methods to measure the piezoelectric effect in NWs consists in a lateral bending of the nanostructure while simultaneously measuring the generated electric potential resulting from the NW deformation. The atomic force microscope (AFM) equipped with an electrical module is a powerful tool for measuring piezoelectric properties of 1D-nanostructures. In fact, this nondestructive characterization technique combines the scanning and deflection measurements capabilities with a nanometer scale resolution and the real-time electrical measurements in usual AFM scanning conditions.

The general principle of measurements is as follows: The conductive AFM tip is brought into contact with the surface of the GaN NWs under a controlled and constant normal force. During the imaging, the tip induces a local bending of the nanowires. In response to this deflection and due to the piezoelectric effect, the NWs generate a voltage which is detected through the conductive AFM tip. Throughout measurements, both the topographic and the electrical signals (output current or output voltage) are recorded continuously and simultaneously. In this specific instrumental configuration, the external electrical system is connected via an Ohmic contact formed between the NWs and the substrate, and a Schottky contact formed between the NW top and the AFM tip, which ensures the charge recuperation for piezo-generation [Liu2008]. No

external voltage is applied and the voltage waveform generated by the NW is observed across a load resistance R_L .

Two different configurations are usually used to perform these measurements: The first one is the scanning configuration (Fig. 3a). In this configuration, the AFM probe scans laterally a vertical array of NWs. The NWs are subjected to an external lateral force resulting from the convolution of the constant normal force and the lateral force resulting from the tip/sample relative displacement. Nanostructures are bended under this external force and an electric field is created inside the nanostructure through the piezoelectric effect. Depending on the distribution of potential within the bended nanowire and the position of the conductive tip on its surface, the Schottky junction formed between the metal tip and the semiconductor NW can be reversely-biased or forward-biased. In this configuration, by soliciting successively each NW over the entire surface scanned by the AFM tip, it is possible to map simultaneously topography and voltage / current peaks. The second configuration is the perpendicular bending configuration (Fig. 3b). In this specific instrumental configuration, the sample is vertically mounted so that the conductive AFM tip applies a local force perpendicular to the free-standing NW at a selected forcing location. This method allows a direct bending of individual NWs and provides a more precise control of the applied force and its point of application. However, because the conductive AFM tip is only in contact with the stretched side of the bended NW, the Schottky diode has to be forward-biased, which implies that for this technique to be effective, a given distribution of the piezoelectric potential within the nanostructure is needed (which in turn depends on the specific characteristics of the nanostructure such as doping and polarity as detailed in section 2.2).

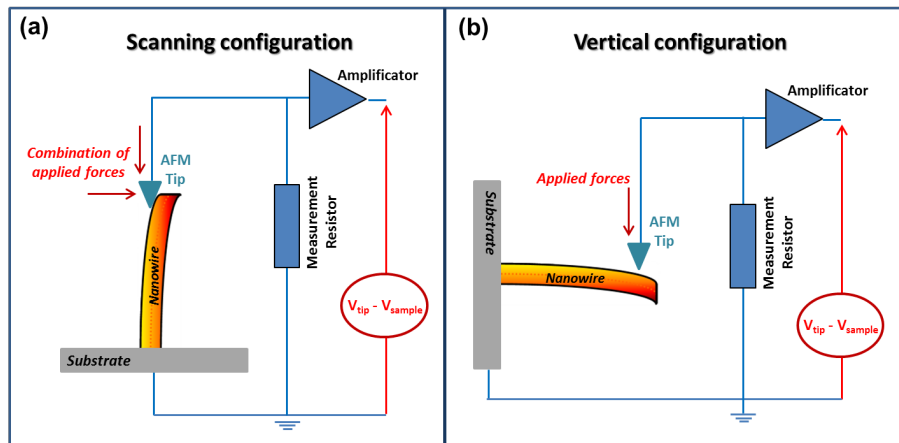


Fig. 3: Schematic representation of atomic force microscope equipped with electrical module for piezoelectric generation measurement for (a) scanning configuration and (b) perpendicular bending configuration.

2.1 Piezogenesis analysis of individual III-N NWs.

The first demonstration of the generation of electrical energy from the mechanical deformation of 1D III-Nitride nanostructures has been done by W. S. Su in 2007, by bending GaN nanorods with an AFM in scanning configuration [Su2007]. Output current with a magnitude of ~ 0.03 nA have been measured as illustrated on figure 4(a). The increase of the output current magnitude with the scanning speed has also been evidenced. The authors assigned this effect to the transfer of kinetic energy resulting from the displacement of the nanorods induced by the scanning of the AFM tip to the elastic energy of the bended nanorods [Su2007].

Contrary to ZnO NWs, which have raised a wide enthusiasm for the piezo-generation application, nitride nanostructures have been much less studied, despite these promising early results. It is probably related to the need for more sophisticated elaboration tools for nitride NW synthesis. It was not until 2010 that nitride nanostructures have started to be actively studied as potentially interesting for the development of piezoelectric generators. The group of Prof. Z. L. Wang, who has introduced the concept of single ZnO NW based nanogenerator [Wang2006], has measured the piezoelectric response of the nitride binary nanostructures, GaN, AlN and InN and of the ternary alloy AlGaN (Figs. 4b-e).

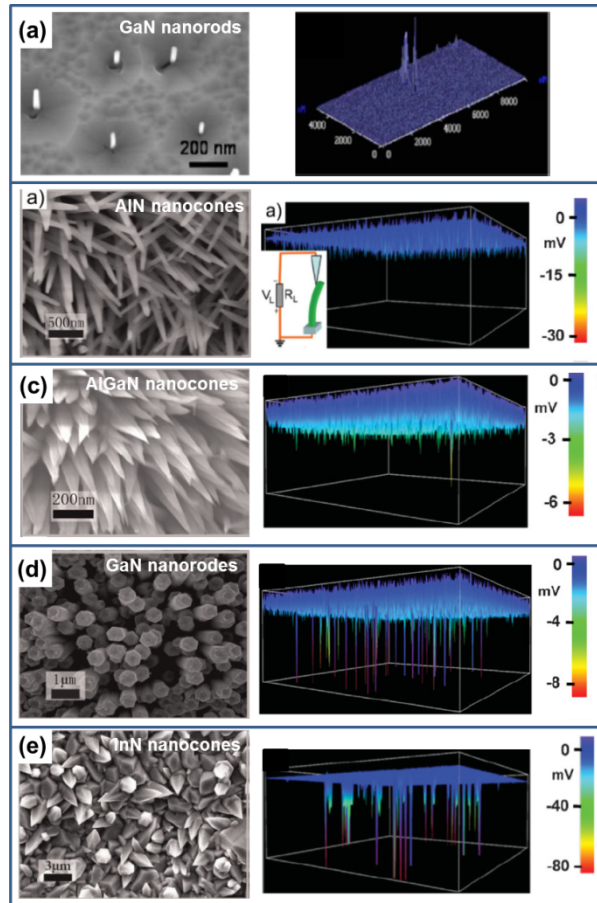


Fig. 4: Scanning Electron Microscope images, Generated output signal mapping and Topographic-electrical profiles of (a) GaN nanorods (reproduced from [Su2007]); (b) AlN nanocones, (c) AlGaN nanocones, (d) GaN nanorods and (e) InN nanocones (reproduced from [Wang2010b]).

Wang and co-workers [Wang2010b] have evidenced the detection of sharp output voltages for all the nitride nanostructures, except for AlN nanocones. Hence, outputs of about 4, 7 and 60 mV for respectively AlGaN, GaN and InN nanocones have been measured using AFM technique. The authors attributed this dispersion in the observed output voltages for the different analyzed nanomaterials to the difference in their conductivity, mainly related to the carrier density. Following their consideration, the AlN nanostructures produced no output signal due to their very high resistivity, while the InN nanocones, due to their high conductivity, generated the largest output voltage. The promise of GaN and InN nanostructures for piezoelectric generation has been confirmed with the measurement of output voltages reaching 300 mV [Chen2012] and 1 V

[Huan2010] per single GaN and InN NWs, respectively (Fig. 5). This output voltage achieved for InN remains until now the highest value for any type of piezoelectric semiconductor nanowire.

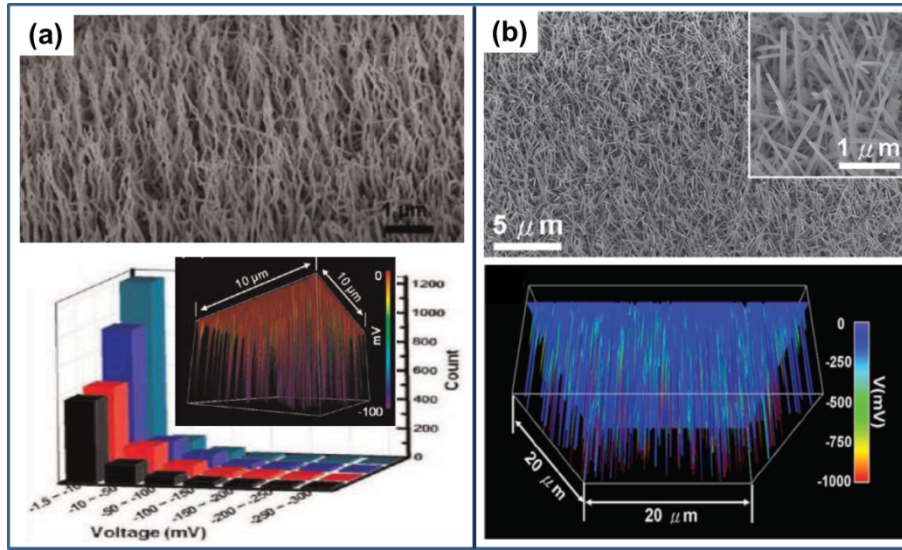


Fig. 5: Scanning Electron Microscope images and generated output signal mapping for (a) GaN and (b) InN NWs, respectively [Reproduced from [Chen2012] and [Huan2010]].

To better understand the piezoelectric response of III-nitride nanostructures, the group of L. Montès has investigated the output voltage generated by intrinsic GaN and GaN/AlN/GaN heterostructured NWs grown by plasma-assisted molecular beam epitaxy [Xu2011]. AFM technique in perpendicular bending configuration was employed. The authors have observed that for both types of NWs, the electrical potential increases as a function of the applied force, as illustrated in figure 6a. The impact of the rate with which the NW is deformed has also been investigated (Fig. 6b), highlighting a good stability and a high reproducibility of the piezo-generated potential.

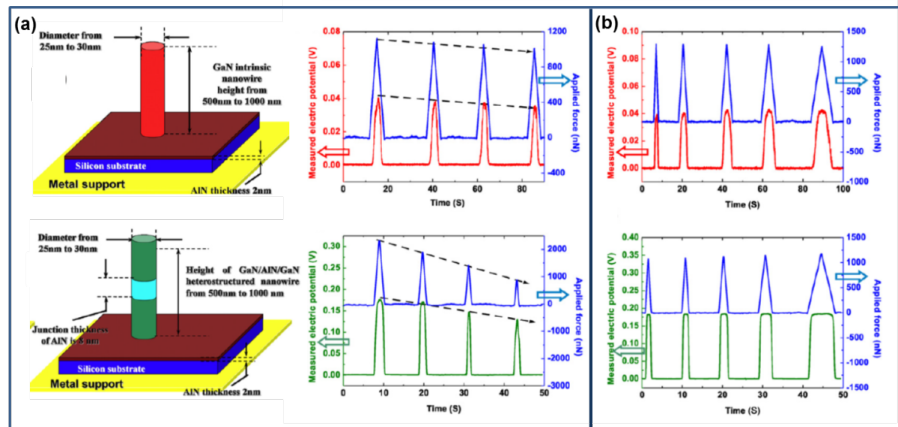


Fig. 6: (a) Schematic illustration of the studied GaN intrinsic nanowires and of GaN/AlN/GaN heterojunction nanowires. Temporal trace of the generated potentials together with the applied force temporal trace. (b) Output signals generated by the NWs for different increase/decrease rate of the applied force. (Reproduced from [Xu2011].)

The perpendicular bending configuration of the AFM technique offers a very good control over the force and the position where this force is applied to the nanostructure. By comparing the two sets of samples under the same experimental conditions ($F_{\text{Applied}} = 250$ nN), the authors observed that the intrinsic GaN NWs generated a potential of the order of 17 mV, while this potential reached 200 mV for heterostructured GaN/AlN NWs (Fig. 7a). In addition, to evidence the impact of the NW structure, the authors experimentally analyzed the relation between the NW deflection and the measured electrical generation (Fig. 7b). The deflection-generation curve can be described as composed of three parts. In the cut-off region, *i.e.* at the beginning of the manipulation, although the deflection is already non zero, the created piezoelectric potential is too small to allow charges to cross the Schottky barrier, and thus no output signal is detected. In the quasi-linear region, the NW deflection induces a sufficient potential to open the Schottky barrier. Output voltages can thus be measured in this regime and are found to increase linearly with the NW deflection. Finally, in the saturation region, the NW deflection becomes very large. The internal piezoelectric potential cannot increase further due to the saturation of the rotation of electric dipoles [Dona2007], and thus the electrical output saturates.

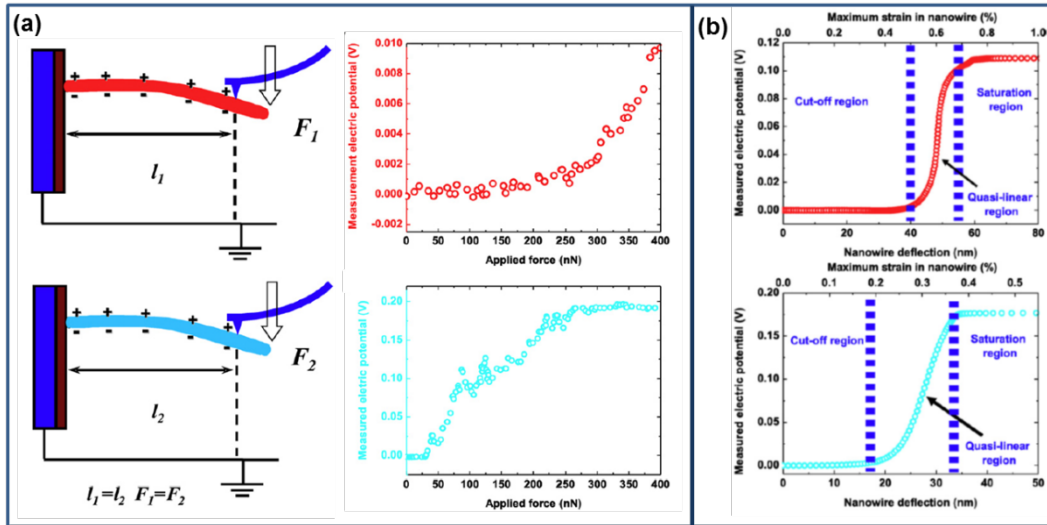


Fig. 7: (a) Output voltage generation as a function of the NW deflection for an intrinsic GaN NW (red) and a GaN/AlN NW (blue). (b) Relation between the NW deflection and the measured electrical generation for an intrinsic GaN NW (red) and a GaN/AlN NW (blue). (Reproduced from [Xu2011].)

Piezoelectric conversion mechanisms of III-nitride NWs were further analyzed by *N. Gogneau et al.* [Gogn2014]. The authors investigated the output voltage generation of a vertical array of intrinsic n-doped GaN NWs as a function of the applied force by using AFM equipped with a Resiscope module in scanning configuration. With this technique, the authors acquired a large measurement statistics, with the output signal distribution reflecting the dimension dispersion of the NWs. However, because of the convolution of the normal force and the lateral force due to the scanning movement of the tip (as illustrated in Figure 3a), the nanostructures are subjected to a higher degree of deformation than when they are stressed by a normal force (perpendicular bending configuration of Figure 3b)). In these conditions, the quantitative analysis of the piezoelectric efficiency of the NWs is technically very complex due to a very strong NW deformation bringing them directly into saturation regime. In order to reduce the NW bending and thus to achieve more reliable electrical measurements, the NWs were mechanically

consolidated by embedding their base part into a PMMA layer (more details can be found in Ref. [Gogn2014]). Figure 8 presents the 3D output voltage map of a partially encapsulated GaN NW array recorded at a constant normal tip force. As *Xu et al.* observed on single nanowires in a quasi-linear region [Xu2011], *Gogneau et al.* showed a statistical enhancement (i.e. enhancement of the maximal value and of the average value) of the signal generated by the ensemble of GaN NWs with increasing the applied force. Two phenomena were put forward to explain this behavior. The first one followed the consideration of *Xu et al.* [Xu2011] on the potential versus NW deflection relation. As the NW deflection increases the resulting internal piezoelectric potential increases, in agreement with theoretical predictions [Gao2007b]. The second phenomenon put forward by *Gogneau et al.* considered the harvesting of the generated energy. The increase of the force applied by the conductive AFM tip leads to a larger surface of the Schottky contact and thus to the improvement of the metal-semiconductor contact stability [Pere2007]. This improved contact allowed then a better harvesting efficiency.

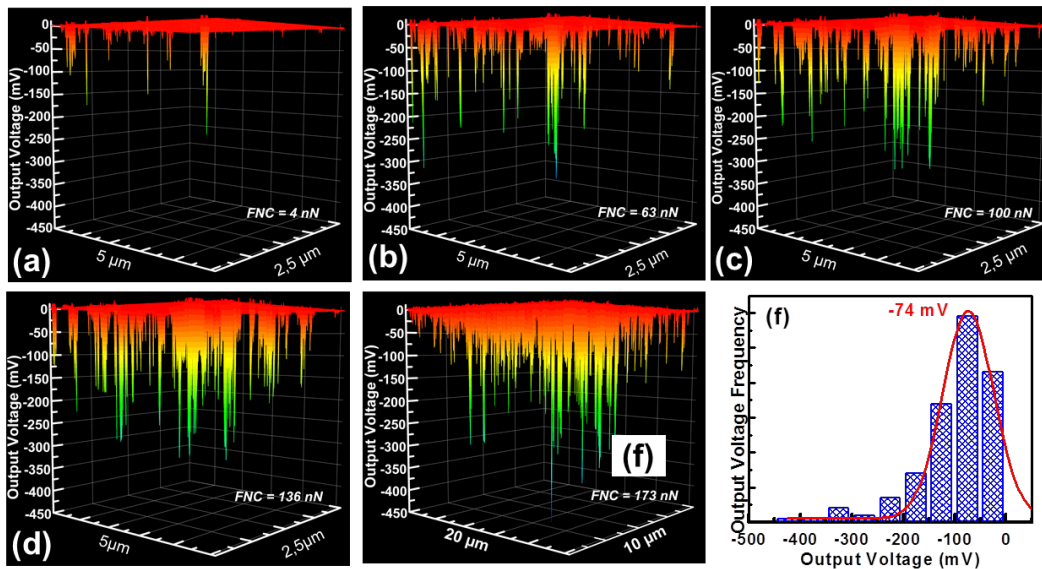


Fig. 8: 3D output voltage map of a vertical array of GaN NWs for different constant normal forces: (a) $F = 4$ nN, (b) $F = 63$ nN, (c) $F = 100$ nN, (d) $F = 136$ nN and (e) $F = 173$ nN. (f) Histogram distribution of the output voltages generated by GaN NWs for $F = 173$ nN. (Reproduced from [Gogn2014].)

From these measurements performed on a large array of GaN NWs, a statistical analysis of the piezo-conversion capacity of the nanostructures was given. An average output voltage of -74 mV and a maximal value of -443 mV per NW were obtained. This latter value largely exceeds the maximum voltage generated by single ZnO NWs (45 mV [Gao2007] and 80 mV [Lu2009] for n-doped and p-doped ZnO NWs, respectively) and represents the highest output voltage reported for GaN NWs. It is noteworthy, that contrary to *Xu et al.* [Xu2011], the electric signal for the largest force measured by *Gogneau et al.* did not reach saturation. This means that the generated output voltage can potentially exceed -443 mV with the increase of the NW deflection.

Several other groups have presented AFM characterizations of single piezoelectric properties of nitride NWs, then demonstrating their promise as nanogenerators [Gogn2014; Huan2010; Xu2011; Wang2010b]. On the basis of these AFM characterizations performed on free-standing

nitride NWs, power densities reaching up to several hundreds of mW/cm^2 [Su2007; Xu2011; Gogn2014; Chen2012b] were estimated. These estimations are usually done for an ideal case under a hypothesis that all NWs show the same piezoconversion (by taking the highest measured output and multiplying by the nanowire density). Although this way of calculating the output power surely leads to its overestimation, it still demonstrates the potential of GaN NWs to generate high output energy. Therefore, III-N NWs can be used as an active material in ultra-compact and integratable renewable energy sources for sustainable, independent and maintenance-free operation of micro-devices.

2.2 Mechanical-electrical conversion mechanisms in III-N NWs.

The enhancement of the mechanical to electrical energy conversion necessary for developing optimized nanowire based piezo-generators requires fundamental understanding of piezoelectric mechanisms taking place inside the nanostructures. Again, the AFM in scanning mode is well suited to analyze the mechanical-electrical conversion mechanisms in individual nanowires. Since this nanometer scale resolved technique allows simultaneous recording of topographic and electrical signals, it is possible to directly correlate the morphology of a given bended NW with its generated voltage peak. This correspondence was established in [Su2007, Gogn2014b] highlighting that the piezo-generation of GaN nanostructures is always observed when the AFM tip gets in contact with the stretched side of the n-doped GaN nanostructures, i.e. when the tip gets in contact with the NW and the deflection starts (Fig. 9).

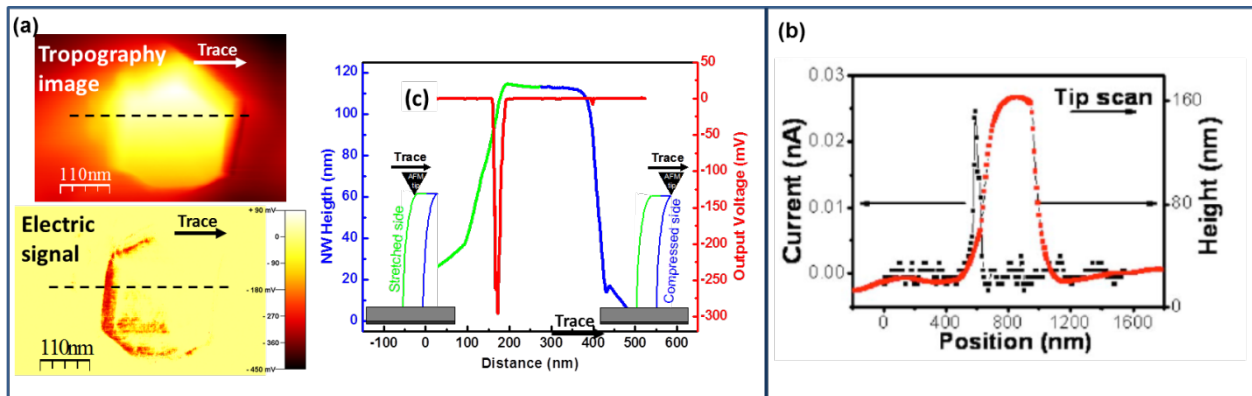


Fig. 9: (a) Topographic and electrical images of GaN NWs and the corresponding topographic and electrical profiles [Gogn2014b]. (b) Topographic profile and the output current for GaN nanorods [Su2007].

The opposite behaviour was observed for n-doped ZnO NWs: in this case, the output signal is generated when the tip is in contact with the compressed side of the NW [Lin2009, Wang2008]. To understand this difference, the piezoelectric properties of the nanomaterials and their doping and polarity characteristics have to be considered. In both cases, the NWs are n-type doped. This electrical characteristic is confirmed by the negative output signals measured by AFM [Lin2009]. The GaN nanostructures are also characterized by being terminated by N-polar surface (N-polarity) as it has been demonstrated by KOH etching [Su2007, Larg2012]. These two specificities are of great importance, since they determine the behaviour of the Schottky diode formed at the interface between the bended GaN NW and the conductive electrode (AFM tip).

When the GaN nanostructure is laterally bended by the AFM tip in scanning configuration, an asymmetric strain is created across the NW. The inner side of the 1D-object is compressed leading to a negative strain, while the outer side is stretched leading to a positive strain, as illustrated in Fig. 10a). As a consequence of this strain field, a piezoelectric polarization (P_{PZ}) appears inside the nanostructure. Under compression, P_{PZ} is oriented anti-parallel to the spontaneous polarization (oriented parallel to the growth direction since the nanostructure are N-polar terminated) and thus oriented opposite to the growth direction, while under stretching, P_{PZ} is parallel to the P_{PS} and aligned with the growth direction. Due to the specific orientation of the piezoelectric polarization in the N-polar GaN NWs, the piezoelectric potential distribution in the wire evolves between V_S^+ at the compressed facet and V_S^- at the stretched facet (Fig. 10b). From this potential distribution through the NW volume, two different situations occur at the Schottky contact (Fig. 10c). When the AFM tip starts to deflect the n-doped GaN nanostructure, the contact between the tip and the stretched side is a positively biased Schottky diode ($\Delta V = V_m - V_S^- > 0$, where V_m is the potential of the metal tip, close to zero in standard conditions). Since the majority carriers are electrons, charges flow across the interface driven by the piezoelectric potential, resulting in an external output voltage detected across the load resistance. By contrast, when the conductive tip reaches the compressed side of the nanostructure, the Schottky diode is reversely biased ($\Delta V = V_m - V_S^+ < 0$) and the charge flow across the interface is blocked, explaining the absence of output voltage.

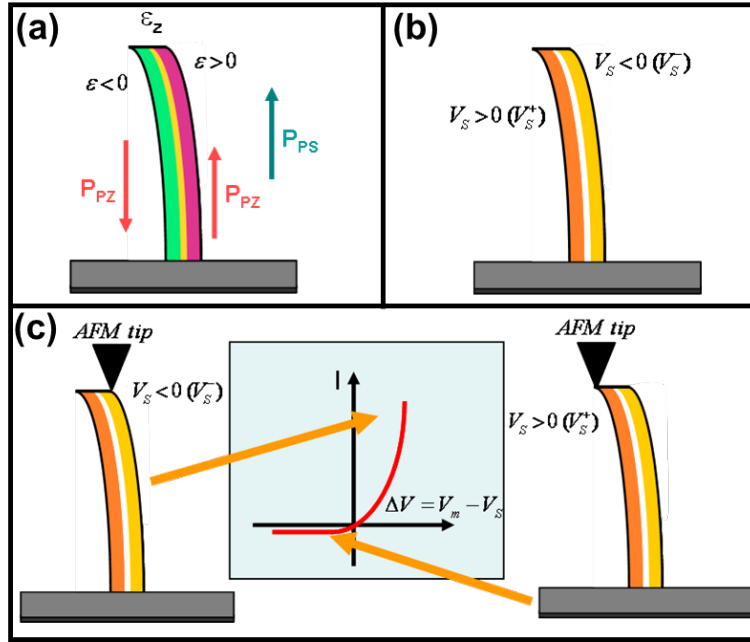


Fig. 10: (a) Strain distribution in a NW bent by conductive AFM tip; (b) Potential distribution in the NW; (c) Biasing condition of the Schottky contact between the NW and the AFM tip for the stretched and compressed sides. The piezopotential distribution illustrated in panel (b) leads to a directly and a reversely biased diode, respectively. (Reproduced from [Gogn2014b].)

By comparison, the n-type doped ZnO nanowires are characterized by metal polarity, i.e. the NWs are terminated by Zn atoms [Wang2003, Wang2007b]. This metal-polarity of the ZnO NWs orients the P_{SP} anti-parallel to the growth direction. The piezoelectric polarization in metal-polar

structures is thus oriented in the opposite direction in comparison with the anion-polarity structures (N-terminated GaN). Consequently, the electric potential through the metal-polar ZnO NWs evolves between V_s^- at the compressed side and V_s^+ at the stretched side. This difference in crystal polarity inducing a difference in potential distribution explains the different generation behaviour between n-doped ZnO and n-doped GaN nanowires.

By considering this mechanism, the piezogenerated of p-doped GaN NWs should be detected on the compressed side of the NWs. In order to verify this point, *Gogneau et al.* have grown and characterized by AFM in scanning mode and array of N-polar Mg-doped GaN NWs [Jamo-sub]. Indeed, the generation as observed only when the AFM tip was in contacted with the compressed side of the NW due to the opposite behaviour of the Schottky diode and the sign of the output voltages was changed to positive as expected for a p-doped structures. This is illustrated in Figure 11.

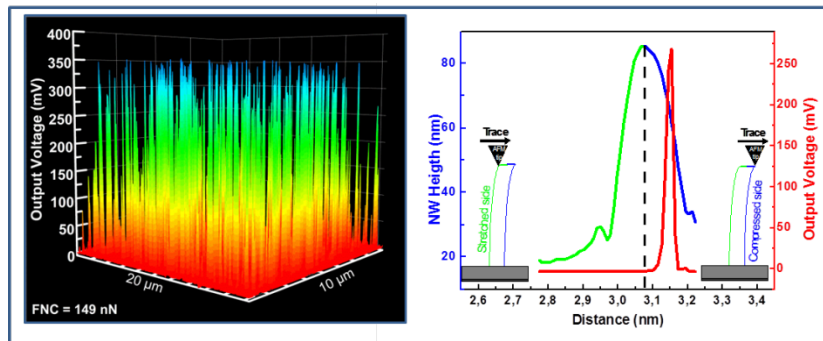


Fig. 11: 3D map of the output voltage generated by p-doped GaN NWs and the correlation between the topographic and electrical signal profiles.

The results described in this section demonstrate that the piezo-generation mechanism crucially depends on the polarity and doping characteristics of the nanostructures, which is of crucial importance to design optimized piezoelectric generators and maximize their conversion efficiency.

3- Piezoelectric generators based on III-N NWs.

Investigations of the piezoelectric energy harvesting by III-nitride individual nanostructures have prepared the development of macroscopic NW-based piezoelectric generators. Today, in spite of the numerous and very promising results obtained on single nanostructures, to the best of our knowledge, only three macroscopic (i.e. with hundreds of micrometres to centimetre dimensions) piezo-generators integrating arrays of III-nitride NWs have been reported in the literature.

The first prototype has been proposed by Prof. Wang and co-workers in 2011 [Lin2011]. It consists of multiple layers of dispersed GaN NWs embedded in polymethyl methacrylate (PMMA), and sandwiched by two metal electrodes of Cr/Au, the ensemble of device being supported by a film of Kapton, as illustrated in figure 12a. To mechanically solicit this generator, the device has been attached to a flexible polystyrene substrate, to which an external force has been applied to bend the generator. Output voltages and output currents up to 1.2 V and 0.16 $\mu\text{A}/\text{cm}^2$ have been measured (Fig. 12b). By considering the dimensions of the devices, namely an

effective size of 5 mm x 5 mm for a thickness of approximately 6.4 μm , a power density of 0.16 mW/cm^3 can be estimated.

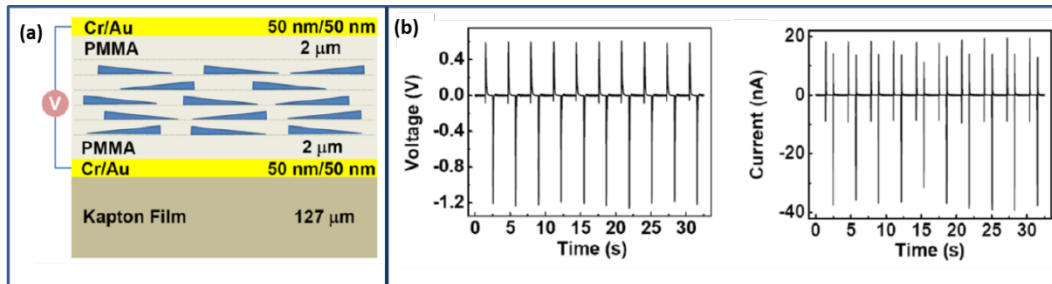


Fig. 12: (a) Schematic illustration of the GaN NW-based piezo-generator. (b) Output voltage (left) and output current (right) generated by the GaN-based piezo-generator with forward connection. (Reproduced from [Lin2011].)

The second demonstrator published very recently [Liu2016] integrates either vertically aligned p-doped InN NWs or intrinsic InN NWs. The nanostructures are embedded into PMMA and the Schottky contact necessary to detect piezoelectric signal is formed between the InN NWs and the MoO_3/Au electrode (Fig. 13a). The piezo-generator devices have been tested under external dynamic strain by anchoring the substrate on a fixed stopper, leaving the top electrode facing outward. By moving up and down the system, a periodic strain was applied. The response of the device to the mechanical solicitation appears under the form of voltage (current) spikes as shown in figure 13b. Open-circuit voltage and short circuit current of ~ 55 mV and ~ 211 nA for p-type piezo-generator and of ~ 85 mV and 80 nA for intrinsic-type piezo-generator have been measured for the same experimental solicitations. The power production of p-type piezo-generator has been found as 70% more than the power production of the intrinsic generator, reflecting better piezoelectric energy conversion efficiency for p-type doped NWs.

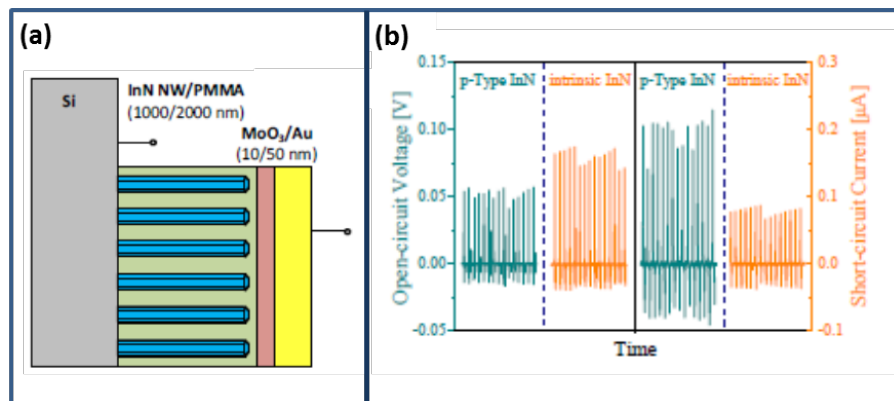


Fig. 13: (a) Schematic diagram of the InN NW-based piezo-generator. (b) Measured open-circuit voltage and short-circuit current of p-type and intrinsic piezo-generators. (Reproduced from [Liu2016].)

A third piezo-generator prototype [Jamo2016] is based on a vertical array of dense GaN NWs. Similar vertical design has been proposed by the group of L. Montes in 2012 [Mont2012], however the device characterization details have not been published. In the work of *Jamond et al*, the device consists of an array of p-doped GaN NWs of several square millimeters in size

embedded into spin-on glass with a Schottky contact for rectification and collection of piezo-generated carriers (Fig. 14a). For p-doped GaN NWs having nitrogen polarity, the top Schottky contact collects carriers under compressive strain. In order to homogeneously strain the active pin-on glass / NW layer, the generator is bended by clamping its two sides and inducing a vertical movement of its central part (Fig. 14b). Due to the difference of thickness between the substrate (350 μm) and the active layer ($\sim 1 \mu\text{m}$), the lateral bending of the device induces stretching of the spin-on glass matrix and, as a consequence of the volume conservation, a thinning of the active layer. The spin-on glass deformation is transmitted to the embedded GaN NWs leading to their homogeneous compression (Fig. 14b). In response to a periodic stressing, the device generates a voltage signal synchronized with the magnitude of the applied force (Fig. 14c). The piezo-generator exhibits a saturated maximal output voltage of about 200 mV, resulting in an output power density of about 12.7 mW/cm^3 . This value settles the new state of the art for piezo-generators integrating arrays of GaN NWs and more generally nitride NWs, and offers promising prospects for the use of GaN NWs for high-efficiency ultra-compact energy harvesters.

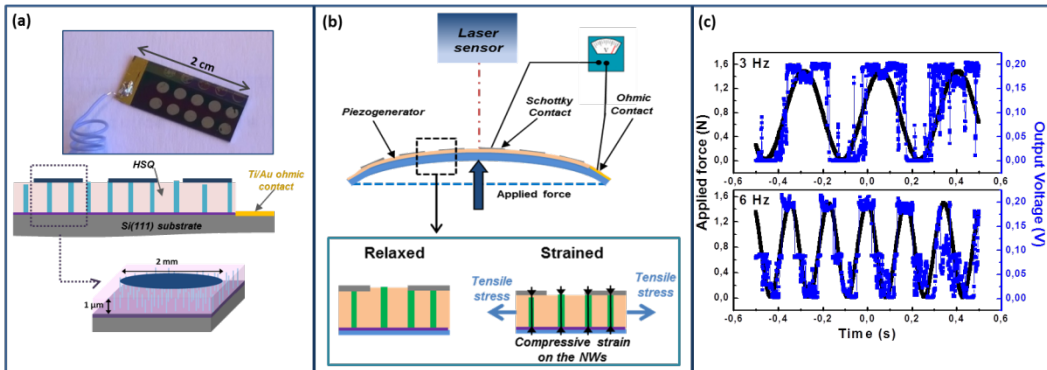


Fig. 14: (a) Optical image and schematization of the piezo-generator fabrication process. (b) Setup used to characterize the piezo-generator. The lateral bending of the generator induces a thinning and thus a compression of the active layer as illustrated. (c) Output voltages generated by the piezo-generator as function of its deformation for a bending cycle rate of 3 Hz (top) and 6 Hz (down).

Conclusion and Perspectives

Piezogenerators based on nitride NWs show promising performance with generated power densities that are already interesting for real world applications (e.g. supplying of remote wireless transceivers etc.). However, the performance of macroscopic devices is still far from the estimations done by extrapolating the best value measured for single nanowires to the nanowire array. It is therefore clear that the optimization of the nanowire properties and in particular a better wire-to-wire homogeneity would allow to enhance the generator performance. NW arrays grown by selective area epitaxy can respond to this need. Impact of different NW characteristics (alloy composition, structure, dimensions, density and conductivity) on the piezoelectric conversion needs also to be explored.

Semiconductor NWs open the possibility for new designs and new functionalities beyond the simple size reduction. Axial or radial heterostructures can be incorporated into NWs can be used

to engineer strain in the active region to further enhance the energy generation. Indeed, when a NW heterostructure contains materials with different lattice constants with layer thicknesses below the critical thickness for relaxation, an elastic strain is created inside the NW modifying the built-in electric fields and the piezoresponse. One example of the usefulness of this strategy is given by the analogy that can be drawn with existing piezo-actuators using prestrained materials to achieve symmetrical voltage response and to improve linearity. Besides, barriers of a higher bandgap material [Xu2011] can be used to localize the free carriers and thus to engineer the internal impedance of the NWs.

Along these lines, it is very likely that future research and development of NW-based piezogenerators will bring these devices to maturity and to the world of real widespread applications as miniature portable energy sources.

Acknowledgments

This work was financially supported by the by EU Horizon 2020 ERC project “NanoHarvest” (Grant 639052), the French National Research Agency through the GANEX program (ANR-11-LABX-0014) and the Region Ile-de-France in the framework of DIM Nano-K.

References

- [Agra2011] Agrawal R., Espinosa H. D. 2011, *Nano Lett.* 11, 786
- [Ardi2012] Ardila G., Hinchet R., Mouis M., Montès L. 2012 *Semiconductor Conference Dresden-Grenoble (ISCDG)*, 2012 International, doi 10.1109/ISCDG.2012.6359985
- [Arma2009] Armand M., Endres F., MacFarlane D. R., Ohno H., Scrosati B., 2009 *Nat Mater.* 8, 621
- [Bern1997] Bernardini F., Fiorentini V., Vanderbilt D. 1997 *Phys. Rev. B.* 56, R100024
- [Bert2007] Bertness K.A., Roshko A., Mansfield L.M., Harvey T.E., Sanford N.A. 1997 *J. Cryst. Growth* 300, 94
- [Brub2011] Brubaker M. D., Levin I., Davydov A. V., Rourke D. M., Sanford N. A., Bright V. M., Bertness K. A. 2001 *J. Appl. Phys.* 110, 053506
- [Chan2005] Lai-Wai Chan H., Li K., Choy C. L. 2005 edited by X M Tao (2005) printed by Woodhead Publishing ISBN :9781855736054
- [Chan2010] Chang C., Tran V.H., Wang J., Fuh Y-K., Lin L. 2010 *Nano Letters* 10, 726
- [Chen2010] Chen X., Xu S., Yao N., Shi Y. 2010 *Nano Lett.* 10, 2133
- [Chen2012] Chen, C.-Y.; Liu, T.-H.; Zhou, Y.; Zhang, Y.; Chueh, Y.-L.; Chu, Y.-H.; He, Jr.-H.; Wang, Z. L. 2012 *Nano Energy* 12, 424.
- [Chen2012b] Chen C-Y., Zhu G., Hu Y., Yu J-W., Song J., Cheng K-Y., Peng L-H., Chou L-J., Wang Z. L. 2012 *ACS Nano* 6 (6), 5687
- [Dona2007] Donald J. L., 2007 New-York: Wiley-Interscience, 124.
- [Feen2002] Feenstra M.R., Northrup J.E., Neugebauer J., 2002 *J. MRS Internet J. Nitride Semicond. Res.* 7, 3
- [Gao2007] Gao P. X. , Song J. , Liu J. L., Wang Z. L. 2007 *Adv. Mater.* 19, 67
- [Gogn2014] Gogneau, N. ; Chretien, P. ; Galopin, E. ; Guilet, S. ; Travers, L. ; Harmand, J.-C. ; Houzé, F. 2014 *Phys. Status Solidi RRL* 8, 414
- [Gogn2014b] Gogneau, N. ; Chretien, P. ; Galopin, E. ; Guilet, S. ; Travers, L. ; Harmand, J.-C. ; Houzé, F. 2014 *Appl. Phys. Lett.* 104, 213105
- [Guy1999] Guy I. L., Muensit S., Goldys E. M. 1999 *Appl. Phys. Lett.* 75 (26), 4133
- [Hans2010] Hansen B. J., Liu Y., Yang R., Wang Z. L. 2010 *ACS Nano* 4, 3647
- [Hinc2014] Hinchet R., Lee S., Ardila G., Montès L., Mouis M., Wang Z. L. 2014 *Adv. Funct. Mater.* 24, 971
- [Hu2011] Hu Y., Xu C., Zhang Y., Lin L., Snyder R. L., Wang Z. L. 2011 *Adv. Mater.* 23, 4068
- [Hu2011b] Hu Y., Zhang Y., Xu C., Lin L., Snyder R. L., Wang Z. L. 2011 *Nano Lett.* 11, 2572
- [Huan2002] Huang D., Reshchikov M.A., Visconti P., Yun F., Baski A.A., King T., Morkoc H., Jasinski J., Liliental-Weber Z., Litton C.W. 2002 *J. Vac. Sci. Technol. B.* 20, 2256
- [Huan2010] Huang C-T., Song J., Tsai C-M., Lee W-F., Lien D-HH., Gao Z., Hao Y., Chen L-J., Wang Z. L. 2010 *Adv. Mater.* 22, 4008
- [Huan2010b] Huang C-T., Song J., Lee W-F., Ding Y., Gao Z., Hao Y., Chen L-J., Wang Z. L. 2010 *J. Am. Chem. Soc.* 132, 4766
- [Jamo2016] N. Jamond, P. Chrétien, F. Houzé, L. Travers, J. C. Harmand, F. Glas, E. Lefeuvre, M. Tchernycheva, N. Gogneau, 2016 *Nanotechnology* 27 325403
- [Jang2002] Jang H.W., Lee J-H., Lee J-L. 2002 *Appl. Phys. Lett.* 80, 3955
- [Ku2012] Ku N-J., Huang J-H., Wang C-H., Fang H-C., Liu C-P. 2012 *Nano Lett.* 12, 562
- [Larg2012] Largeau L., Galopin E., Gogneau N., Travers L., Glas F., Harmand J-C. 2012 *Cryst. Growth Des.* 12, 2724

- [Lee2011] Lee M., Bae J., Lee J., Lee C. S., Hong S., Wang Z. L. 2011 *Energy Environ. Sci.* 4, 3359
- [Lee2014] Lee S., Hinchet R., Lee Y., Yang Y., Lin Z-H., Ardila G., Montès L., Mouis M., Wang Z. L. 2014 *Adv. Func. Mat.* 24 (8), 1163
- [Li2010] Li Z. , Zhu G. , Yang R. , Wang A. C., Wang Z. L. 2010 *Adv. Mater.* 22, 2534
- [Lin2008] Lin, Y. F.; Song, J.; Ding, Y.; Lu, S.-Y.; Wang, Z. L. 2008 *Appl. Phys. Lett.* 92, 022105
- [Lin2009] Lin S.S., Song J.H., Lu Y.F., Wang Z.L. 2009 *Nanotechnol.* 20, 365703
- [Lin2011] Lin L., Lai C. H., Hu Y., Zhang Y., Wang X., Xu C., Snyder R. L., Chen L. J., Wang Z. L. 2011 *Nanotechnol.* 22, 475401
- [Liu2008] Liu J., Fei P., Song J., Wang X., Lao C., Tummala R., Wang Z.L. 2008 *Nano Lett.* 8, 328
- [Liu2016] Liu G., Zhao S., Henderson R. D. E., Leonenko Z., Abdel-Raman A., Mi Z., Ban D. 2016 *Nanoscale*, 8, 2097
- [Lu2009] Lu M. P., Song J., Lu M. Y., Chen M. T., Gao Y., Chen L. J., Wang Z. L. 2009 *Nano Lett.* 9, 1223
- [Mill2008] Miller J. R., Simon P. 2008 *Science* 321, 651
- [Mina2012] Minary-Jolandan M., Bernal R. A., Kuljanishvili I., Parpoil V., Espinosa H. D. 2012 *Nano Lett.* 12, 970
- [Mome2010] Momeni K., Odegard G. M., Yassar R. S. 2010 *J. Appl. Phys.* 108, 114303
- [Mont2012] Montes L., Xu X., Potie A., Bercu B., Hinchet R., Rochette F., Ardila G., Morfouli P., Mouis M., Baron T., Salem B., Songmuang R., “Piezoresistivity and Piezoresistance in Semiconductor nanowires for sensors and energy devices“, *Semiconductor Nanowires Based Sensors GDR*, November 13-14 2012, Rennes, France ; Montes L., Tao R., Hinchet R., Ardila G., Mouis M., Silveira-Stein S., Hauser D., Faucherand P., Savelli G., “Energy Harvesting from Nanostructures”, *3rd International Symposium on Next-Generation Electronics (ISNE)*, Taiwan May 07-10, 2014.
- [Pan2010] Pan C., Fang Y., Wu H., Ahmad M., Luo Z., Li Q., Xie J., Yan X., Wu L., Wang Z.L. Zhu J. 2010 *Adv. Mater.* 22, 5388
- [Pan2011] Pan C., Li Z., Guo W., Zhu J., Wang Z. L. 2011 *Angew. Chem. Int. Ed.* 50, 11192
- [Pere2007] Perea-Garcia B., Zuniga-Perez J., Munoz-Sanjose V., Colchero J., Palacios-Lidon E. 2007 *Nano Lett.* 7, 1505
- [Schn2011] Schneegans O., Chrétien P., Houzé F., French Patent FR 10 01940, 05/05/2010, international PCT WO 2011/138738, 10/11/2011
- [Salo2014] Salomon S., Eymery J., Pauliac-Vaujour E. 2014 *Nanotechnology* 25(37), 375502
- [Song2007] Songmuang R., Landré O., Daudin B. 2007 *Appl. Phys. Lett.* 91, 251902
- [Su2007] Su W. S., Chen Y. F., Hsiao C. L., Tu L. W. 2007 *Appl. Phys. Lett.* 90, 063110
- [Wang2003] Wang Z.L., Kong X.Y., Zuo J.M. 2003 *Phys. Rev. Lett.* 91, 185502
- [Wang2006] Wang Z. L., Song J. H. 2006 *Science* 312, 242
- [Wang2007] Wang X., Song J., Liu J., Wang Z. L. 2007 *Science* 316, 102
- [Wang2007b] Wang Z. L. 2007 *Materials Today* 10, 20
- [Wang2008] Wang Z. L. 2008 *Adv. Funct. Mater.* 18, 3553
- [Wang2010] Wang, Z.; Hu, J.; Suryavanshi, A. P.; Yum, K.; Yu, M.-F. 2010 *Nano Lett.* 10, 2966
- [Wang2010b] Wang X., Song J., Zhang F., He C., Hu Z., Wang Z. L. 2010 *Adv. Mater.* 22, 2155
- [Wen2015] Wen X., Wu W., Pan C., Hu Y., Yang Q., Wang Z. L. 2015 *Nano Energy* 14, 276
- [Xu2008] Xu S., Wei Y. G., Liu J., Yang R., Wang Z. L. 2008 *Nano Lett.* 8, 4027
- [Xu2010] Xu S., Qin Y., Xu C., Wei Y., Yang R., Wang Z. L. 2010 *Nat. Nanotechnol.* 5, 366

- [Xu2011] Xu X., Potié A., Songmuang R., Lee J. W., Bercu B., Baron T., Salem B. L., Montès L. 2011 *Nanotechnol.* 22, 105704
- [Yang2009] Yang R. S., Qin Y., Dai L. M., Wang Z. L. 2009 *Nat. Nanotechnol.* 4, 34
- [Yang2010] Yang P., Yan R., Fardy M. 2010 *Nano Lett.* 10, 1529
- [Zhao2004] Zhao M. H., Wang Z. L., Mao S. X. 2004 *Nano Lett.* 4, 587
- [Zhou2012] Zhou Y. S., Hinchet R., Yang Y., Ardila G., Sangmuang R., Zhang F., Zhang Y., Han W., Pradel K., Montès L., Mouis M., Wang Z. L. 2013 *Adv. Mater* 13, 883.
- [Zhou2012b] Zhou, Y. S.; Han, W.; Rai, S. C.; Zhang, Y.; Ding, Y.; Pan, C.; Zhang, F.; Zhou, W.; Wang, Z. L. 2012 *ACS Nano* 2012, 6, 6478
- [Zhou2013] Zhou Y. S., Hinchet R., Yang Y., Ardila G., Songmuang R., Zhang F., Zhang Y., Han W., Pradel K., Montès L., Mouis M., Wang Z. L. 2013 *Advanced Materials* 25 (6), 883
- [Zhu2010] Zhu G. A., Yang R. S., Wang S. H., Wang Z. L. 2010 *Nano Lett.* 10, 3151
- [Zhu2012] Zhu G. , Wang A. C. , Liu Y. , Zhou Y. , Wang Z. L. 2012 *Nano Lett.* 12, 3086